INTERNATIONAL JOURNAL OF
ENERGY AND ENVIRONMENT

Volume 6, Issue 3, 2015 pp.287-298

Journal homepage: www.IJEE.IEEFoundation.org

A site-specific design of a fixed-pitch fixed-speed wind turbine blade with multiple airfoils as design variable

Arturo Del Valle-Carrasco[1], Delia J. Valles-Rosales[1], Luis C. Mendez[2], Alejandro Alvarado-Iniesta[2]

[1] New Mexico State University, Department of Industrial Engineering, MSC 4230/ECIII, PO Box 30001, Las Cruces NM, 88003-8001, USA.
[2] Autonomous University of Ciudad Juarez, Department of Industrial Engineering and Manufacturing Av. Del Charro, 450 Nte, Ciudad Juarez, Chihuahua, 32315, Mexico.

Abstract
This study seeks to optimize a fixed-pitch fixed speed (FPFS) wind turbine blade's performance using the chord, twist and the use of 3 different airfoils with varying relative thickness as design variables for the maximization of the Annual Energy Production for the wind profile of Roswell NM. A baseline design of the blade starts with a replica of the Phase VI blade utilized in a NASA-Ames experiment and a Matlab script utilizes the Blade Element Momentum Theory (BEM) for the aerodynamic analysis. The SQP method for Local Search are used to exploit the model utilizing the Phase VI design as a starting point which contains the S809 airfoil with a 0.21 relative thickness for the complete blade. Optimization results reduced the relative thickness of the airfoils to 0.17 and an increase of 36% in energy production was observed using this method.

Keywords: BEM; SQP; Optimization; HAWT; Wind energy.

1. Introduction

Global warming along with depletion of fossil fuels have created changes in energy policies in countries around the globe. Several countries in Western Europe are developing wind energy capacities aggressively such as Denmark having 30% of its electricity supplied by wind energy, Portugal 18%, Ireland 16%, Germany 10%, and the US presently consists of only 4.4%. However, the U.S. Department of Energy [1] stated a goal of reaching a 20% electricity production generated by wind resources by the year 2030.

There are two main types of wind turbines: the Vertical Axis Wind Turbine (VAWT) and the Horizontal Axis Wind Turbine (HAWT). Of the two topologies the most popular with manufacturers is the two or three-bladed HAWT due to its cost effectiveness in reliability, acoustics and efficiency [2]. Some HAWTs possess a blade pitching mechanism and therefore are known as a variable-pitch turbine, whereas their counterparts lacking this mechanism are known as fixed-pitch (FP) [3]. An additional variation is related to the speed at which the rotor spins: the two topologies are the fixed-speed (FS) and the variable-speed (VS) wind turbines. A variety of wind turbine which does not pitch its blades and has a fixed speed rotor is known as a fixed-pitch fixed-speed (FPFS) wind turbine. Compared to a FPVS turbine which use permanent magnet synchronous generators requiring complex electronics for grid

connections, the FPFS have the advantage of being robust, reliable and of lower cost than the variable-speed [4]. A FPFS will yield a maximum coefficient of power at only one given wind speed unlike a VS rotor, however research has shown that for high values of the Weibull's shape parameter of a wind profile, the FPFS turbines have competitive Annual Energy Production (AEP), to about 88% of its variable-speed version [5].

Wind turbine design optimization has been an ongoing research in academia and in the industrial practice during the last couple of decades. Previous optimization efforts have focused in an optimization of the twist and the chord of a given FPFS wind turbine with the objective to maximize the energy production [6-8]. Additional efforts have been performed in the area of airfoil optimization to improve the aerodynamic efficiency of the HAWT's airfoils for VS rotors [17-19]. For example Fuglsang (2004) designed the RISO family of airfoils to maximize the coefficient of torque and lift and minimize roughness [9], other studies modified the leading edge for roughness sensitivity [10, 11].

Some wind turbine airfoils are designed to have a high C_l/C_d and at the same time a high C_l for a given *alpha-design* angle of attack [12]. The optimizations of the C_l/C_d for a given *alpha-design* can be useful for an airfoil that is to be fitted in a VP or a VS turbine, since a control strategy can be implemented where the pitch or speed of the rotor is modified to maximize the exposure of the airfoil's optimum *alphas*. This is not the case in a FPFS which may not modify either parameter and hence its airfoils will be exposed at its optimum *alpha-design* for only one given wind speed, and consequently function at suboptimum levels for any other wind speed.

The Phase VI wind turbine will be utilized as a starting point design of the optimization process. In 2001, The U.S. National Renewable Energy Laboratory published experimental data [13] for the Phase VI wind turbine performed in the NASA-Ames wind tunnel located in Moffet Field, California. The wind turbine consists of 2-blades with 5.03-meter radius with chord and twist variable along the blade and a 3-degree pitch. The airfoil is the S809 and it is the same along the blade with a relative thickness of 0.21; the rotational velocity is 72 RPM [14].

The energy production of the rotor is simulated using BEM theory as in Manwell [15]; BEM Theory is widely used in the literature and in the industry to simulate the energy production of rotors for the energy optimization of wind turbines [7, 16-18]. The design proposed consists of a 2-bladed FPFS rotor with 3 different airfoils with variable relative thickness described by four Bezier curves; the chord and the twist are also modeled using one Bezier curve each. In particular the airfoils will have variable relative thickness with possible values ranging from 0.16 to 0.40 ratio *thickness/chord length (t/c)*. Since there are three airfoils, each one of them will be utilized for one third of the total length of the blade and will be referred as root, mid-section and tip airfoil.

The flow analysis of the airfoils is calculated with Drela's XFOIL [19] code to find their coefficients of lift and drag. XFOIL is a method used widely in the literature for the design of low speed airfoils [20-23]. Since BEM theory requires an extrapolation of the coefficients of lift and drag from -180 to 180 degrees the AERODAS method by Spera [24] was utilized to perform the extrapolation.

It is the aim of this study to investigate the impact of chord, twist with the addition of airfoil design and their relative thickness in the energy production of a FPFS wind turbine. The article is organized as follows: Section 2 explains the objective function to be maximized, Section 3 elaborates the design variables and constraints; Section 4 describes the methodology utilized for maximization of the objective. Finally, Section 5 and 6 close with results and conclusions of the study.

2. Objective function

The objective function to maximize will be the AEP using the wind profile for the location of Roswell NM. The data consists of hourly data wind speed obtained from the National Oceanic and Atmospheric Administration [25] station name Roswell Industrial Air Park, NM US with station ID GHCND:USW00023009 for the periods of January 1st 2010 to December 31st 2010. The data is characterized with a Weibull probability density function (*pdf*):

$$f_w(U) = (k/c)\cdot(U/c)^{k-1}\exp[-(U/c)^k] \tag{1}$$

where U represents the speed of the wind and k and c are the shape and scale parameters of the distribution. After a calculation of the Coefficient of Power (C_p) curve by BEM theory, the AEP can be obtained with the formula established by Hau [26]

$$AEP = 8760 \times \tfrac{1}{2}\eta\rho A\int_{cut-in}^{cut-out} U^3 C_p(U) \times f_w(U)dU \quad (2)$$

where η is the transmission efficiency of the wind turbine including the mechanical and electrical efficiency which is considered 85% in this study, ρ is the air density 1.062 kg/m^3, A=79.485m^2 corresponds to the area spanned by the rotor, the cut-in and cut-out speeds are 5 and 25 m/s.

3. Design variables and constraints

The shape of the blade is determined by the airfoil contour, the chord, and the twist distribution of each section of the blade. In order to achieve smooth distributions of the chord and the twist, two Bezier curves are used to describe them; for the airfoil shape four composite Bezier curves will be used to determine their shape.

The design proposed consists of a 2-bladed FPFS rotor with three different airfoils each described by four Bezier curves. Since three airfoils are proposed, each will be used for one third of the total length of the blade. In particular the first airfoil occupies the length from the root at 1.257 to 2.51m; the second airfoil from a length of 2.51 to 3.77m and the third airfoil from a length of 3.77m to the tip of the blade at 5.03m; they are referred as root, mid, and tip airfoils for simplicity.

3.1 Chord and twist distributions

Bezier curves require four control points each containing two coordinates, in this case the first coordinate represents the position of the point along the radius and the second represents either the chord or the twist values. Thus, the points that define the chord's Bezier are:

$$(r_{ci}, c_i) \quad \text{for} \quad i = 1,2,3,4 \quad (3)$$

And the twist's by

$$(r_{ci}, t_i) \quad \text{for} \quad i = 1,2,3,4 \quad (4)$$

The chord is constrained to be a decreasing curve for structural reasons, hence the constraint obtained is:

$$1.257 = r_{ch1} \le r_{ch2} \le r_{ch3} \le r_{ch4} = 5.03 \quad (5)$$

$$0.75 \ge c_1 \ge c_2 \ge c_3 \ge c_4 \ge 0 \quad (6)$$

In Eq. (6) a limit in the length of the chord is set at 0.75m, and each subsequent chord coordinate must be decreasing to achieve a blade that tapers down.

The Phase VI has twist values ranging from 25 to 3 degrees from the root to the tip respectively, in this study a larger set of values will be allowed for exploration resulting in the constraints

$$1.257 = r_{t1} \quad \text{and} \quad r_{t4} = 5.03 \quad (7)$$

$$1.257 \le r_{t2}, r_{t3} \le 5.03 \quad (8)$$

$$0 \le t_i \le 40 \quad \text{for} \quad i = 1,2,3,4 \quad (9)$$

An additional constraint is concerned with the distribution of the chord not being larger than the Phase VI's as it would be undesirable to create a design that produces more energy at the expense of a wider blade i.e. more costly; thus the chord distribution of the design will necessarily be constrained to be 'under' that of the Phase VI. This results in the constraint:

$$\int_{1.257}^{5.03} Bezier((r_{c1}, c_1),...,((r_{c4}, c_4))dr \le \int_{1.257}^{5.03} Bezier(PhaseVI - chord)dr = 2.06 \quad (10)$$

3.2 Airfoils

A variation in several of the dimension in the airfoils will be allowed in the study including relative thickness. As it was previously established by Grasso [12] a variation in relative thickness is recommended for the inner part of the blade to be larger than the outer part for structural requirements since they have a higher priority in the inside of the blade. In this study relative thickness values between 16% to 40% will be explored for the designed airfoil. The structural integrity of the blade is not considered in the scope of this study

For the parameterization of the airfoils, four composite Bezier curves are used as shown in Figure 1; The first curve is formed by points 1-4, the second curve by points 4-7, the third by 7-10, and the fourth curve is composed of points 10, 11, 12, and back to point 1. Points 1, 4, 7, and 10 are shared by adjacent curves. In addition, Point 1 and Point 7 are always fixed at (1,0) and (0,0) respectively.

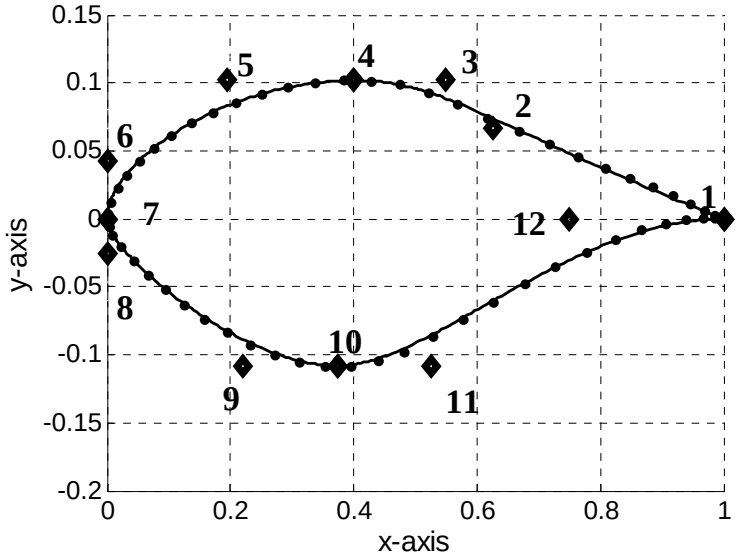

Figure 1. Parametrization of S809 with Beziers

Each *x* and *y-coordinates* of control points not fixed have upper and lower bound constraints. Table 1 sets the lower and upper limits for each coordinates of the airfoils' control points; *x-coordinates* in point 6 and 8 are fixed at zero to achieve a smooth transition between curves connecting at Point 7; the same case applies to Points 3 and 5 *y-coordinates* in which the values are set equal to Point 4, as this yields a smooth transition between curves connecting at Point 4.

Table 1. Control Points upper and lower bounds

	x-Coordinates		y-coordinates	
Point No.	min	max	min	max
Point 2	0.525	0.9	0.04	0.15
Point 3	0.52	0.675	Same as Pt. 4	
Point 4	Fixed at 0.4		0.08	0.2
Point 5	0.1075	0.2725	Same as Pt. 4	
Point 6	Fixed at 0		0.02	0.10
Point 8	Fixed at 0		-0.10	-0.01
Point 9	0.12	0.3	Same as Pt. 10	
Point 10	Fixed at 0.37425		-0.20	-0.08
Point 11	0.475	0.6375	Same as Pt. 10	
Point 12	0.65	0.85	-0.10	0.07

The problem yields six variables for the chord, six for the twist, and each airfoil requires the use of twelve variables for each of the three airfoils i.e. root, midsection and tip areas; a total of 48 variables are considered in the problem.

Airfoils performance is also affected by Reynolds number (Re) defined as [15]

$$\mathrm{Re} = \rho U_{rel} c / \mu \tag{11}$$

where c is the chord length of the airfoil, U_{REL} is the relative wind velocity to the airfoil, and μ is the viscosity of the airfoil. An estimation of the Reynolds number in the blade's mid-section of the baseline Phase VI blade which has a chord length of 0.54m needs to be established in order to set a baseline of analysis

Considering that the most of the energy gathered from the wind profile in the area of Roswell are at wind speeds of 10m/s as shown in Figure 2 an analysis of the Reynolds number in the baseline blade will be made for 5, 7.5 and 10m/s.

In Table 2 the Reynold numbers for the midsection of the preliminary blade as estimated from the given wind speeds are calculated. This speed calculation is based in the triangle of speeds from Blade Element Theory. In order to obtain the quantity U_{REL} necessary for Eq. (1) the formula

$$U_{REL} = sqrt(U^2 + U_{TAN}^2) \tag{12}$$

Is used, in which

$$U_{TAN} = \Omega \cdot r \tag{13}$$

Since the rotor speed is constant at 72 RPM the Reynolds number of the HAWT do not vary significantly, which is in the range of 900,000 to 950,000. To simplify the optimization process the design Reynolds number is chosen as 925,000. However it must be clarified that this technique would not be appropriate for other topologies of wind turbines such as variable speed where these values vary significantly.

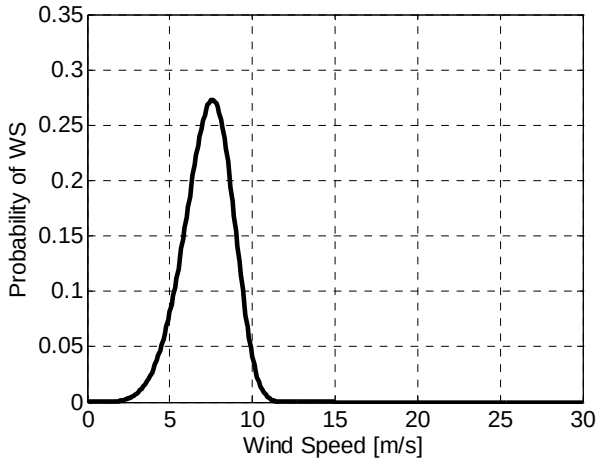

Figure 2. Wind pdf of Roswell, NM

Table 2. Estimated Reynolds at wind speeds

$U(m/s)$	$U_{TAN}(m/s)$	$U_{REL}(m/s)$	Re
5	23.7	24.2	899,224
7.5	23.7	24.9	922,859
10	23.7	25.7	954,966

4. Methodology

In order to calculate the AEP of a given design a set of scripts were written in MATLAB 2014a. It consists on a function which receives a candidate design in the form of a vector containing the control points of the chord, twist, and all airfoils. All lower and upper bounds were mapped to the interval [0, 1]

to add simplicity in the coding process. The script receives the vector of the candidate design and a Bezier function will generate the curve distributions for the chord, twist and the three airfoils. Using a DOS shell from Matlab the code executes XFOIL to acquire flow analysis for angles of attack from -8 to 22 at a Re = 925,000 then its results are saved in a text file. A MATLAB script reads the previously written text files and extracts information required for the extrapolation of the coefficients of lift and drag from -180 to 180 degrees by utilizing the AERODAS model as designed by Spera [24]. An example of an extrapolation of the coefficients is shown in Figure 3.

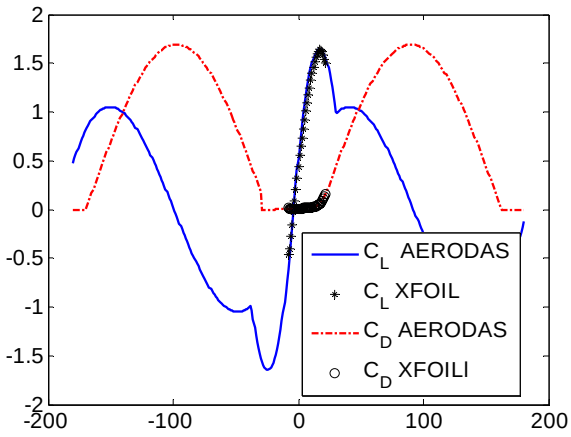

Figure 3. AERODAS extrapolation

A BEM script is executed and returns a Cp curve for the wind speeds 5m/s to 25m/s; finally the formula in Eq. (2) is implemented to calculate the final result of the objective function. A diagram is shown on the process utilized in the calculation of the AEP in Figure 4.

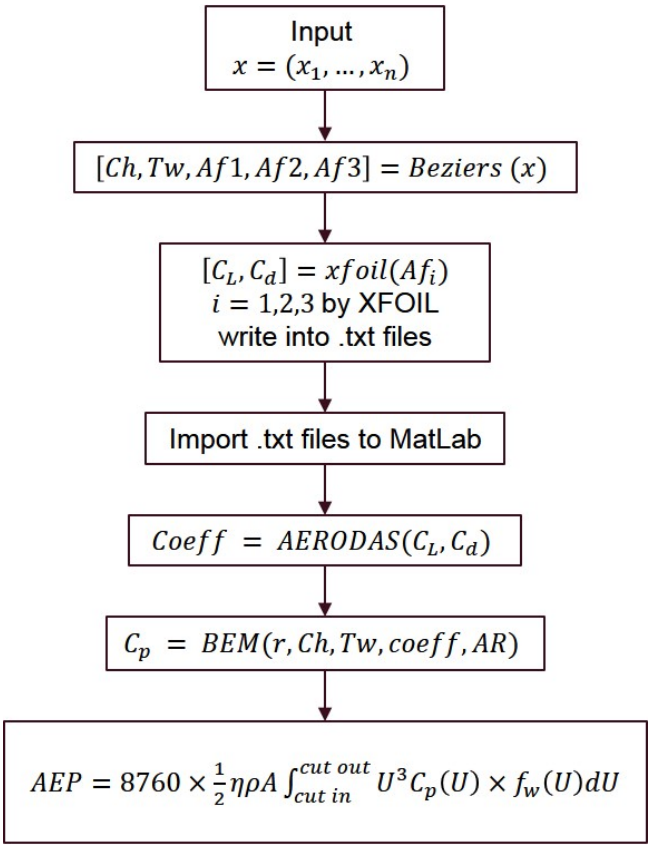

Figure 4. Calculation procedure for the AEP

The SQP algorithm in Matlab with a relative step of 0.15 for the finite difference step was implemented on the AEP calculation for an optimization of the design. The starting point for the search was the design of the Phase VI wind turbine blade in which the airfoils are the S809 for all sections of the blade with a relative thickness of 0.21. The optimization took 18 iterations with a total of 1672 function evaluations.

5. Results

The results of the optimized design increase the AEP by 36%. The initial AEP for the Phase VI blade for the area of Roswell NM yields a value of 4.4x107 W-h. For the designed blade the total energy production is of $6.0x10^7$ W-h.

The most important constraint is for the chord to not have a larger profile than that of the Phase VI as this would yield a design with an increased cost. In Figure 5, it is shown that chords for the optimized blade and the Phase VI are almost identical with the optimized being slightly smaller.

Figure 6 presents also twists for both blades where the optimized has a smaller profile for the twist with decreasing values of around 18 to a little over 0 degrees in the tip of the blade.

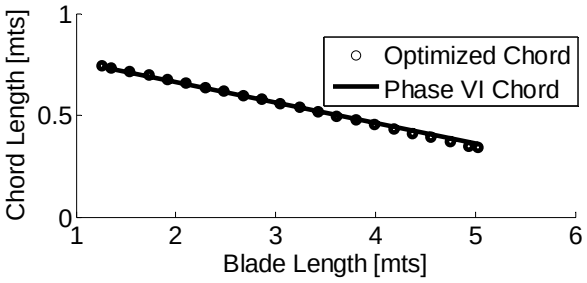

Figure 5. Chords of the optimized and Phase VI

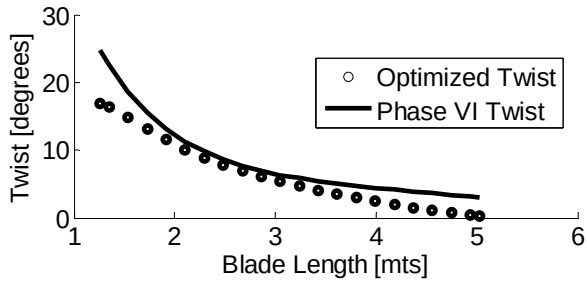

Figure 6. Twists of the optimized and Phase VI

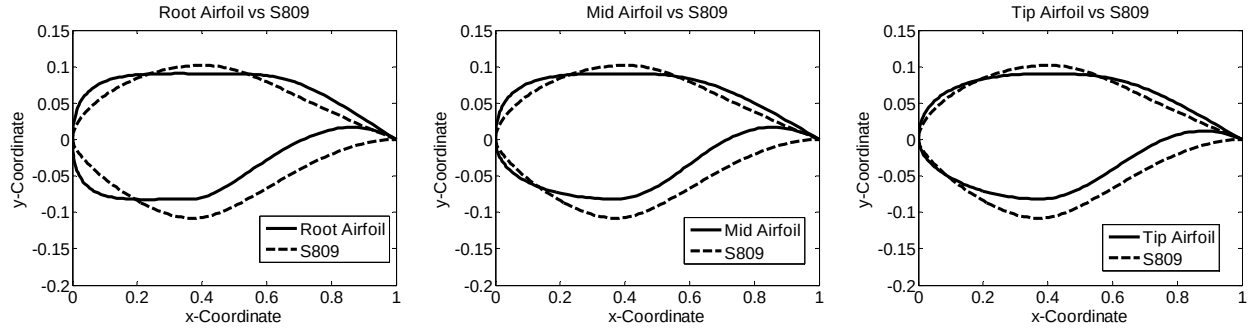

Figure 7. Airfoils for the root, mid-section and tip airfoils compared against the S809

The relative thickness of the three airfoils were identical after the optimization process going from a value of around 0.21 which corresponds to the S809 to a value of exactly 0.1722 for all of them (Figure 7). This indicates as expected that the optimization will tend to shift to smaller thicknesses for better aerodynamic properties, however this may compromise the structural integrity of the blade if the lower bounds of this parameter reaches low levels.

Figure 8 shows the coefficients of lift of the optimized airfoils obtained from XFOIL, with values always above those of the S809 airfoil (Re=9.25x10^6), also their *alpha* value at stall are higher than the S809's. The Cp curves of all the designed airfoils for an angle of attack at seven degrees is shown in Figure 9 where they show similar shapes as they share several points in common in account of their identical relative thickness

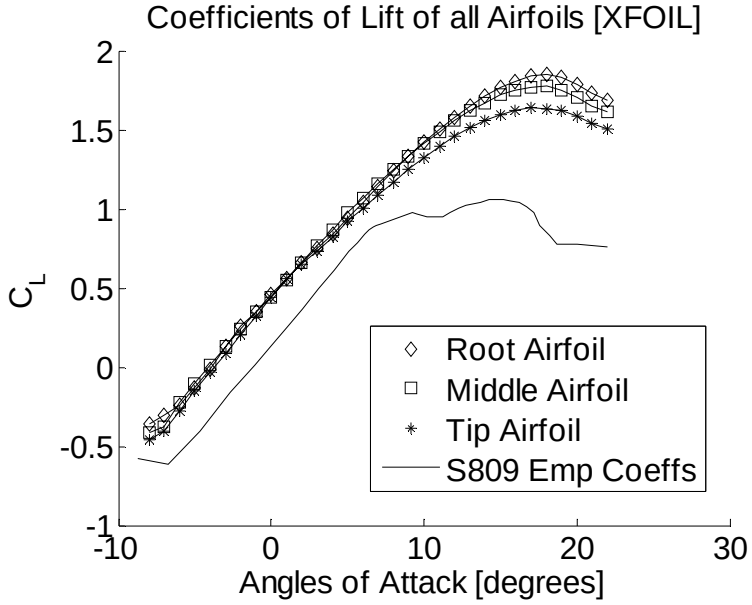

Figure 8. Coefficients of Lift at Re= 925,000 for designed airfoils and S809

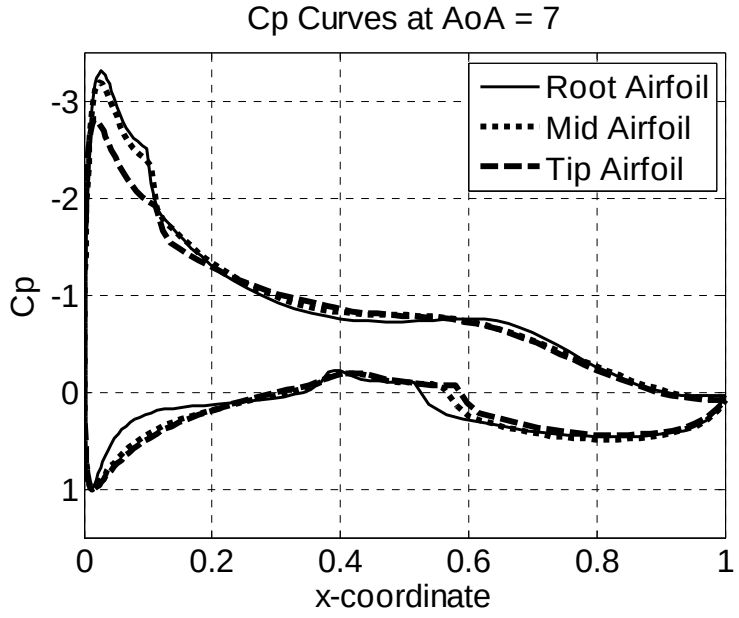

Figure 9. Cp Curves at 7 degrees

The ratio *Cl /Cd* of the designed airfoils have values of 63.7, 67.7, and 69.4 for the root, midsection and the tip respectively at angles of attack 8, 7, and 7 degrees. Figure 10 shows a plot of the C_l /C_d for the designed airfoils and the S809. The plot indicates that the designed airfoils have a maximum aerodynamic efficiency lower than that of the S809's, however they have larger values for a larger range of the angles of attack. This is a possible indication that airfoils suited for a FPFS should have *Cl /Cd* curves which do not necessarily require a high max*(Cl /Cd)* as illustrated by the S809's, but instead a flatter curve with non-steep decrements are of preference. This points to the idea that higher aerodynamic efficiency are required for a large range of *alpha* values since the lack of pitching mechanism and rotor speed variability will expose it to several *alphas* depending on wind speed changes.

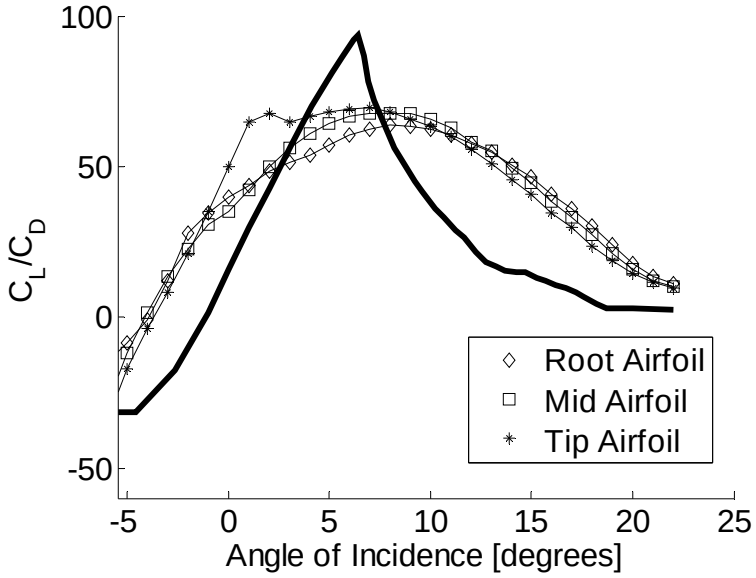

Figure 10. C_l/C_d for the designed airfoils and the S809

A contrast of the energy harvested by each airfoil in the optimized blade is presented in Figure 11 compared against the Phase VI's energy output. Every airfoil curve for outer sections is higher than the inner segments as they can capture more energy on account of their radial position. Figure 11 shows the mid-section of the optimized blade generates almost an identical amount of energy as that of the Phase VI outer portion of the blade which suggests a good optimization level for the design.

A plot of the energy produced by the entire blade for every wind speed is shown in Figure 12, which shows that for wind speeds of 11 m/s and lower most of the energy is harvested.

For a better analysis of this information a plot of the angles of attack in every segment of the blade is shown in Figure 13, which shows that the angles of attack in the airfoils go from around 2 degrees to around 22. This indicates that instead of a maximization of the C_l/C_d of the airfoil for a given *alpha-design*, the optimization should be implemented for a range of angles of attack which would likely hit the blade for the majority wind speeds.

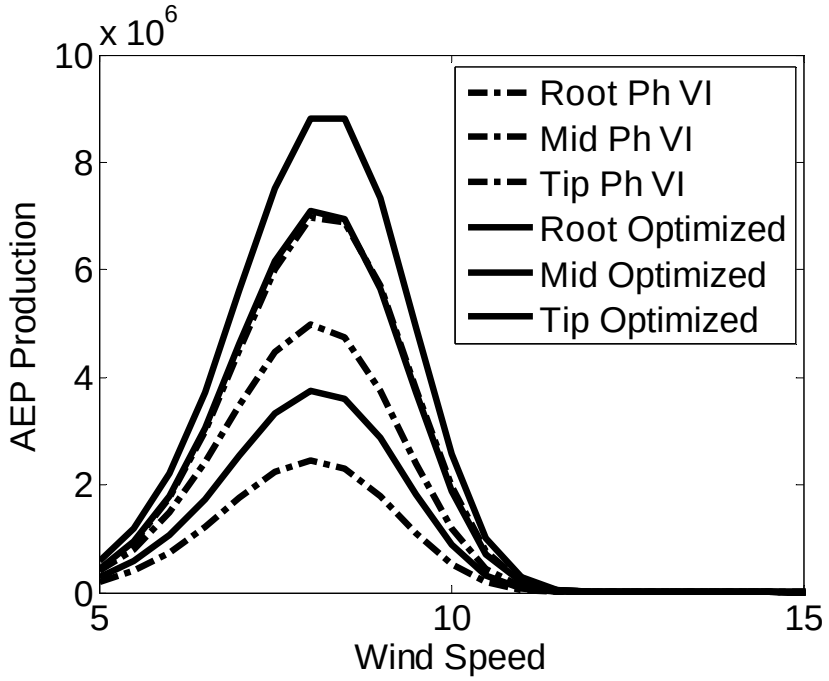

Figure 11. Energy yields by the root, mid-section and tip portion of the optimized and the Phase VI blade depending on wind speeds

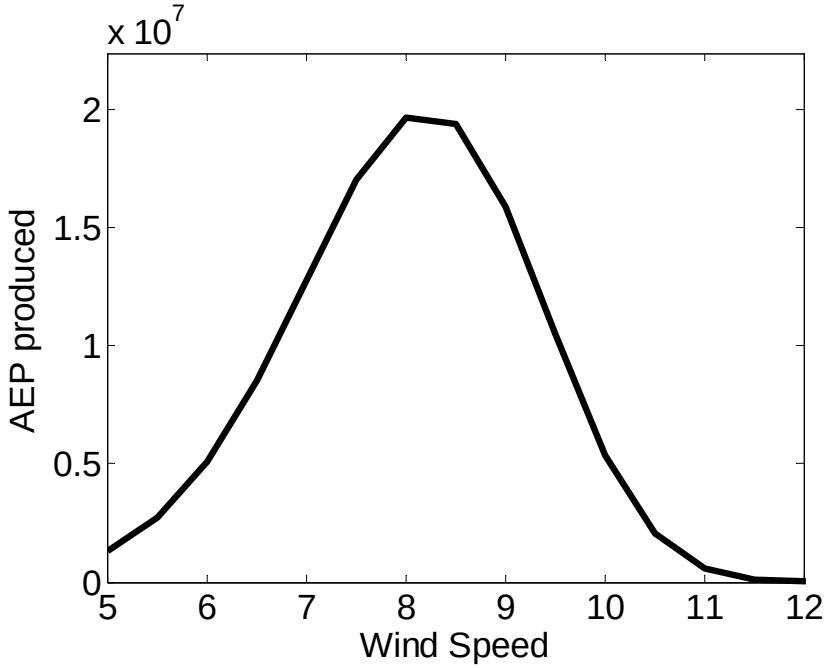

Figure 12 Energy produced by the blade at different wind speeds

For a better analysis of this information a plot of the angles of attack in every segment of the blade is shown in Figure 13, which shows that the angles of attack in the airfoils go from around 2 degrees to around 22. This indicates that instead of a maximization of the C_l/C_d of the airfoil for a given *alpha-design*, the optimization should be implemented for a range of angles of attack which would likely hit the blade for the majority wind speeds.

Finally, in Figure 14 the C_p curve generated by the optimized blade is shown against that of the Phase VI's. The plot shows the optimized curve is above the baseline design for every wind speed, which means it will be more efficient for any variation of wind profiles.

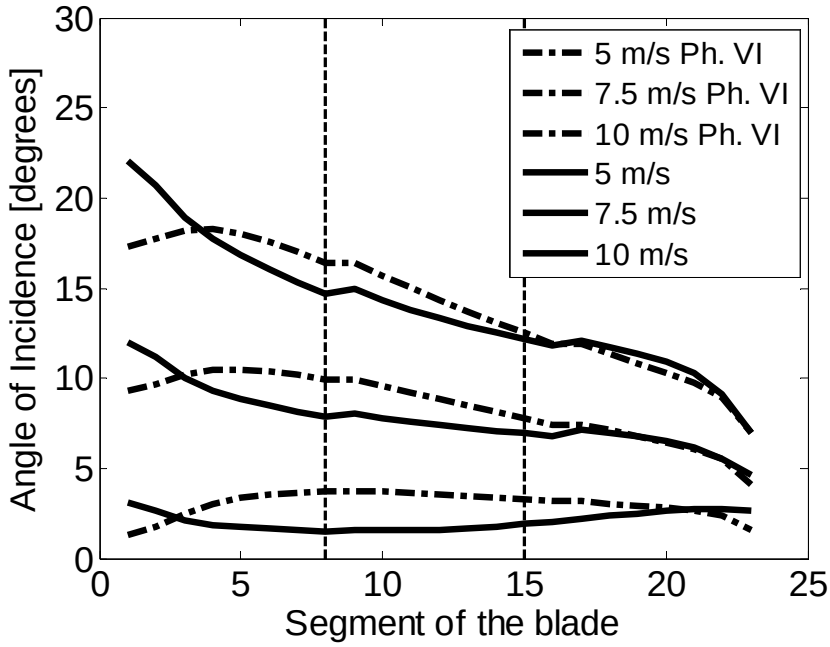

Figure 13. Angle of attacks at 5, 7.5 and 10 m/s at given blade segments

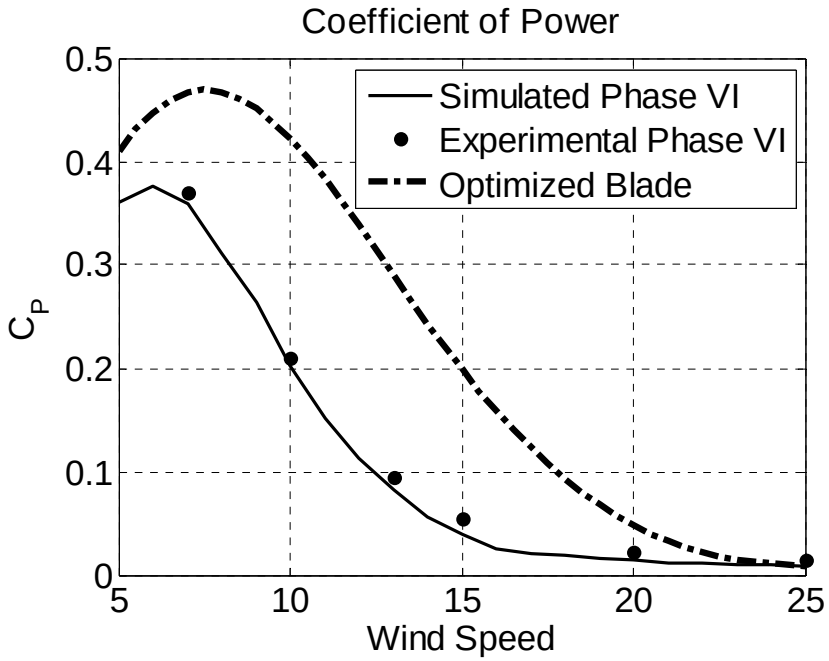

Figure 14. Coefficient of Power for Phase VI and the designed blade

6. Conclusions

A FPFS wind turbine was optimized in this study to maximize the Annual Energy Production using the chord, twist, and three different airfoils with variable relative thickness as design variables which where modeled utilizing Bezier curves. The wind profile used data obtained from the NOAA for a station located in the city of Roswell, NM. A baseline design for the optimization of this blade starts with the Phase VI developed in the NASA-Ames experiment which consists of a variable twist and chord with a length of 5.03m and containing the S809 airfoil with a 0.21 relative thickness. The simulation of the energy production of the rotors was conducted by the use of the Blade Element Momentum Theory and the SQP method was employed to optimize the given design. The results returned three airfoils with identical relative thickness at 0.17, less than the S809's; also a smaller twist and chord distributions were found to be optimal if compared to the Phase VI blade. In total the design blade has an AEP increase of 36%.

The designed airfoils had curves of coefficients of lift above those of the S809 airfoil. Furthermore, the plot of the C_l/C_d indicated that the S809 had a higher max(C_l/C_d) for a given *alpha* than those of the three designed airfoils. However, the aerodynamic efficiency of the S809 quickly goes below those of the designed airfoils. This result is congruent with the fact that a FPFS turbine is always exposed to a wide range of angles of attack as wind speeds change. Taking into account that several airfoils in the past have been designed by maximizing the C_l/C_d --as they are fitted for VP or VS systems-- suggests that a maximization in the aerodynamic efficiency for one *alpha-design* is not be the best technique to implement for a FPFS wind turbine.

Acknowledgement

The authors are grateful to the United States Department of Agriculture (USDA) for their support to this project via the BuildinG a Regional Energy and Educational Network (BGREEN) grant.

References

[1] R. Wiser, 2012 Wind technologies market report. (2014).
[2] R.W. Thresher, D.M. Dodge, Trends in the evolution of wind turbine generator configurations and systems. Wind Energy 1 (1998) 70-86.
[3] F.D. Bianchi, H. De Battista, R.J. Mantz, Wind turbine control systems: principles, modelling and gain scheduling design, Springer, 2006.

[4] D. Saheb-Koussa, M. Haddadi, M. Belhamel, S. Hadji, S. Nouredine, Modeling and simulation of the fixed-speed WECS (wind energy conversion system): application to the Algerian Sahara area. Energy 35 (2010) 4116-4125.
[5] G. Venkatesh, S. Kulkarni, Energy yield of passive stall regulated fixed speed wind turbine with optimal rotor speed. Electric power systems research 76 (2006) 1019-1026.
[6] X. Liu, Y. Chen, Z. Ye, Optimization model for rotor blades of horizontal axis wind turbines. Frontiers of Mechanical Engineering in China 2 (2007) 483-488.
[7] X. Liu, L. Wang, X. Tang, Optimized linearization of chord and twist angle profiles for fixed-pitch fixed-speed wind turbine blades. Renewable Energy 57 (2013) 111-119.
[8] E. Minisci, M. Campobasso, M. Dell'Antonio, A. Montecucco, M. Vasile, Multi-disciplinary robust design of variable speed wind turbines, Conferenza EUROGEN, Settembre, 2011.
[9] P. Fuglsang, C. Bak, M. Gaunaa, I. Antoniou, Design and verification of the Risø-B1 airfoil family for wind turbines. Journal of solar energy engineering 126 (2004) 1002-1010.
[10] C. Bak, P. Fuglsang, Modification of the NACA 632-415 leading edge for better aerodynamic performance. Journal of solar energy engineering 124 (2002) 327-334.
[11] W. Timmer, R. Van Rooij, Summary of the Delft University wind turbine dedicated airfoils. Journal of Solar Energy Engineering 125 (2003) 488-496.
[12] F. Grasso, Development of thick airfoils for wind turbines. Journal of Aircraft 50 (2013) 975-981.
[13] C. Lindenburg, Investigation into rotor blade aerodynamics. Netherlands Society for Energy and the Environment, Paper ECN-C-03-025 (2003).
[14] M. Hansen, Documentation of code and airfoil data used for the NREL 10-m wind turbine. ROTABEM-DTU, November (2000).
[15] J. Manwell, J. McGowan, A. Rogers, Wind energy explained: theory, design and application., 2nd Edition ed., Wiley, New York, NY, USA, 2009.
[16] G.R. Fischer, T. Kipouros, A.M. Savill, Multi-objective optimisation of horizontal axis wind turbine structure and energy production using aerofoil and blade properties as design variables. Renewable Energy 62 (2014) 506-515.
[17] R. Lanzafame, M. Messina, Design and performance of a double-pitch wind turbine with non-twisted blades. Renewable Energy 34 (2009) 1413-1420.
[18] X. Liu, Blade Design Optimisation for Fixed-Pitch Fixed-Speed Wind Turbines. ISRN Renewable Energy 2012 (2012).
[19] M. Drela, XFOIL: An analysis and design system for low Reynolds number airfoils, Low Reynolds number aerodynamics, Springer, 1989, pp. 1-12.
[20] B. Bavanish, K. Thyagarajan, Optimization of power coefficient on a horizontal axis wind turbine using bem theory. Renewable and Sustainable Energy Reviews 26 (2013) 169-182.
[21] T. Kim, S. Lee, H. Kim, S. Lee, Design of low noise airfoil with high aerodynamic performance for use on small wind turbines. Science in China Series E: Technological Sciences 53 (2010) 75-79.
[22] X. Li, K. Yang, J. Bai, J. Xu, A method to evaluate the overall performance of the CAS-W1 airfoils for wind turbines. Journal of Renewable and Sustainable Energy 5 (2013) 063118.
[23] N. Mittal, S. Ahmed, N. Tenguria, EVALUATION OF PERFORMANCE OF HORIZONTAL AXIS WIND TURBINE BLADES BASED ON OPTIMAL ROTOR THEORY. Journal of Urban and Environmental Engineering 5 (2011) 15-23.
[24] D.A. Spera, Models of lift and drag coefficients of stalled and unstalled airfoils in wind turbines and wind tunnels. National Aeronautics and Space Administration, NASA/CR-2008-215434 (2008).
[25] National Oceanic and Atmospheric Administration. (2014, January). Retrieved from http://www.ncdc.noaa.gov
[26] E. Hau, Wind turbines: fundamentals, technologies, application, economics, 2006, in: L. Hansen (Ed.), Springer, 2006.

